doi:10.1093/brain/awab118 BRAIN 2021: 144; 2199–2213 | 2199

BRAIN
ORIGINAL ARTICLE

The Developing Human Connectome Project: typical and disrupted perinatal functional connectivity

Michael Eyre,[1] Sean P. Fitzgibbon,[2] Judit Ciarrusta,[1,3] Lucilio Cordero-Grande,[1] Anthony N. Price,[1] Tanya Poppe,[1] Andreas Schuh,[4] Emer Hughes,[1] Camilla O'Keeffe,[1] Jakki Brandon,[1] Daniel Cromb,[1] Katy Vecchiato,[1,3] Jesper Andersson,[2] Eugene P. Duff,[2,5] Serena J. Counsell,[1] Stephen M. Smith,[2] Daniel Rueckert,[4] Joseph V. Hajnal,[1] Tomoki Arichi,[1,6] Jonathan O'Muircheartaigh,[1,3] Dafnis Batalle[1,3,†] and A. David Edwards[1,†]

[†]These authors contributed equally to this work.

The Developing Human Connectome Project is an Open Science project that provides the first large sample of neonatal functional MRI data with high temporal and spatial resolution. These data enable mapping of intrinsic functional connectivity between spatially distributed brain regions under normal and adverse perinatal circumstances, offering a framework to study the ontogeny of large-scale brain organization in humans. Here, we characterize in unprecedented detail the maturation and integrity of resting state networks (RSNs) at term-equivalent age in 337 infants (including 65 born preterm).

First, we applied group independent component analysis to define 11 RSNs in term-born infants scanned at 43.5–44.5 weeks postmenstrual age (PMA). Adult-like topography was observed in RSNs encompassing primary sensorimotor, visual and auditory cortices. Among six higher-order, association RSNs, analogues of the adult networks for language and ocular control were identified, but a complete default mode network precursor was not. Next, we regressed the subject-level datasets from an independent cohort of infants scanned at 37–43.5 weeks PMA against the group-level RSNs to test for the effects of age, sex and preterm birth. Brain mapping in term-born infants revealed areas of positive association with age across four of six association RSNs, indicating active maturation in functional connectivity from 37 to 43.5 weeks PMA. Female infants showed increased connectivity in inferotemporal regions of the visual association network. Preterm birth was associated with striking impairments of functional connectivity across all RSNs in a dose-dependent manner; conversely, connectivity of the superior parietal lobules within the lateral motor network was abnormally increased in preterm infants, suggesting a possible mechanism for specific difficulties such as developmental coordination disorder, which occur frequently in preterm children.

Overall, we found a robust, modular, symmetrical functional brain organization at normal term age. A complete set of adult-equivalent primary RSNs is already instated, alongside emerging connectivity in immature association RSNs, consistent with a primary-to-higher order ontogenetic sequence of brain development. The early developmental disruption imposed by preterm birth is associated with extensive alterations in functional connectivity.

Received January 29, 2020. Revised December 11, 2020. Accepted December 16, 2020. Advance access publication March 18, 2021
© The Author(s) (2021). Published by Oxford University Press on behalf of the Guarantors of Brain.
This is an Open Access article distributed under the terms of the Creative Commons Attribution License (http://creativecommons.org/licenses/by/4.0/), which permits unrestricted reuse, distribution, and reproduction in any medium, provided the original work is properly cited.

Downloaded from https://academic.oup.com/brain/article/144/7/2199/6178274 by Imperial College London Library user on 10 September 2021

1 Centre for the Developing Brain, School of Biomedical Engineering and Imaging Sciences, King's College London, London SE1 7EH, UK
2 Wellcome Centre for Integrative Neuroimaging (WIN FMRIB), University of Oxford, Oxford OX3 9DU, UK
3 Department of Forensic and Neurodevelopmental Science, Institute of Psychiatry, Psychology and Neuroscience, King's College London, London SE5 8AF, UK
4 Biomedical Image Analysis Group, Imperial College London, London SW7 2AZ, UK
5 Department of Paediatrics, University of Oxford, Oxford OX3 9DU, UK
6 Department of Bioengineering, Imperial College London, London SW7 2AZ, UK

Correspondence to: Dr Dafnis Batalle
Department of Forensic and Neurodevelopmental Science
Institute of Psychiatry, Psychology and Neuroscience
King's College London
16, De Crespigny Park, SE5 8AF, London, UK
E-mail: dafnis.batalle@kcl.ac.uk

Correspondence may also be addressed to: Professor David Edwards
Centre for the Developing Brain
School of Biomedical Engineering and Imaging Sciences
King's College London, London SE1 7EH, UK
E-mail: ad.edwards@kcl.ac.uk

Keywords: neonatology; brain development; functional connectivity; resting-state connectivity; neuroanatomy

Abbreviations: dHCP = Developing Human Connectome Project; DMN = default mode network; ICA = independent component analysis; PMA = postmenstrual age; rs-fMRI = resting state functional MRI; RSN = resting state network; TEA = term-equivalent age

Introduction

The Developing Human Connectome Project (dHCP) is an Open Science project funded by the European Research Council to provide a large dataset of functional and structural brain images from 20 to 44 weeks of gestational age. This enables the characterization of 4D (three spatial dimensions and time) connectivity maps, which map the trajectories of human brain development to improve understanding of normal development and allow earlier detection and intervention for neurological and psychological disorders.

This paper analyses functional connectivity at the time of normal birth in infants born at term and preterm. Temporal coherences in the blood oxygen level-dependent (BOLD) contrast measured with resting state functional MRI (rs-fMRI) can be spatio-temporally decomposed into resting state networks (RSNs),[1,2] predominantly at low frequency (<0.1 Hz),[3] distinct from cardiovascular signal.[4] Whilst RSNs have been extensively and robustly characterized in the mature brain, previous studies of RSN development in newborn infants have been limited by smaller sample sizes. The dHCP provides the first high quality, large-scale, 4D dataset of functional connectivity at this critical period of development, enabling us to address two key questions. First, are higher order RSNs such as the default mode network (DMN)[5] instated with adult topology in the neonatal period? Some find analogues of these at term-equivalent age (TEA)[6–10] while others locate their origin in later infancy or early childhood, contemporaneous with the emergence of the higher cognitive abilities these networks are believed to support.[11,12] Second, what is the effect of preterm birth on RSN development? Preterm birth is associated with significant risk for enduring neurodevelopmental and psychiatric problems in later life,[13–16] even in the absence of overt structural brain injury during the preterm period. Various alterations in the complexity, scope, strength and efficiency of functional connectivity in preterm-at-term infants have been reported[9,10,17–19]; however, the majority of studies lack the large numbers of control subjects required to characterize these effects with precision.

The mature adult RSNs are well characterized, with high intra-subject reproducibility,[20,21] largely consistent topology across healthy subjects, and anatomical mapping that reinforces both structural and task-functional MRI-derived parcellations of the cortex.[22] The identification of functional MRI-RSN signatures associated with disease offers considerable translational potential due to rs-fMRI's relatively straightforward and widely used acquisition, whole-brain coverage, and high spatial resolution compared to other functional imaging methods. The achievement of this in the immature brain requires a complete account of RSN ontogeny. The developing CNS shows spontaneous, patterned, correlated intrinsic activity from early prenatal life (reviewed in Blankenship and Feller,[23] Keunen *et al.*[24] and Vasung *et al.*[25]); immature RSNs can be identified from as early as 26 weeks postmenstrual age (PMA) in the preterm infant.[6,9] By TEA, RSNs encompassing brain regions serving primary functions (sensorimotor, auditory, visual) are clearly apparent in mature configuration in both term and preterm-born infants[6–8,10–12,26] and show minimal change in infancy, while higher order association networks appear to be largely fragmented at TEA, with studies suggesting that they synchronize into complete adult-like core structure in the first year (DMN, dorsal attention network) or second year (salience network, bilateral frontoparietal networks) of life.[11,12] Importantly, TEA is not a single time point but rather a window encompassing a critical period of brain development in which there is intense myelination of white matter (reviewed in Dubois *et al.*[27]) and rapid expansion in both the size and gyrification of the cerebral cortex.[28,29] Dense sampling

Downloaded from https://academic.oup.com/brain/article/144/7/2199/6178274 by Imperial College London Library user on 10 September 2021

across the age range is therefore required to map the associated changes in functional connectivity.

Here, we apply a data-driven approach to 337 rs-fMRI datasets acquired in term and preterm infants between 37 and 44.5 weeks PMA. We first defined a normative set of RSNs in a subsample of term-born infants scanned at 43.5–44.5 weeks PMA using probabilistic independent component analysis (ICA).[30] ICA is a dimensionality reduction technique that decomposes data into a set of components with maximal statistical independence; applied to rs-fMRI, ICA can reveal large-scale brain networks without requirement for a predefined model of network structure. We then regressed subject-level data from term and preterm infants scanned at 37–43.5 weeks PMA against these networks. The resulting whole-brain correlation maps enabled us to both characterize the ontogeny of individual RSNs, and investigate the influence of prematurity on cortical functional connectivity. We hypothesized that primary sensorimotor RSNs would be well established at TEA, while higher order RSNs would be immature and emerging; and that preterm birth would be associated with reduced functional connectivity at TEA.

Materials and methods

Subjects

Research participants were prospectively recruited as part of the dHCP, an observational, cross-sectional Open Science programme approved by the UK National Research Ethics Authority (14/LO/1169). Written consent was obtained from all participating families prior to imaging. Term-born infants were recruited from the postnatal wards and approached on the basis of being clinically well. Preterm-born infants were recruited from the neonatal unit and postnatal wards. Infants were not approached for study inclusion if there was a history of severe compromise at birth requiring prolonged resuscitation, a diagnosed chromosomal abnormality or any contraindication to MRI scanning (e.g. due to incompatible implants). No infants included in the final study group required treatment for clinically significant brain injury. We selected 416 structural-functional datasets acquired at TEA from the 2019 (second) dHCP data release. Only infants scanned at 37–44.5 weeks PMA in term-born infants, or 37–43.5 weeks PMA in preterm-born infants, were considered for inclusion. One infant was included twice because of the two datasets being acquired at different ages; only the second dataset was used. Thirty-five infants were excluded because of a history of neurodevelopmental disorder in a first-degree relative. Forty-three were excluded because of motion (see the 'Functional data preprocessing' section). The final study population therefore consisted of 337 infants, divided into three groups: (i) term-born infants scanned at 43.5–44.5 weeks PMA, who were used to define the normative set of RSNs and excluded from all subsequent subject-level analyses; and the remaining infants scanned at 37–43.5 weeks PMA, including both (ii) term-born; and (iii) preterm-born infants (Table 1). No infants in the preterm study group had major brain injury such as periventricular leukomalacia, grade 3 or 4 intraventricular haemorrhage, major intracerebral haemorrhage, or ischaemic focal brain lesions. As is commonly seen in preterm infants, there was evidence of mild pathologies including 15 (23%) with a history of grade 1 or 2 intraventricular haemorrhage; 10 (15%) with small cerebellar haemorrhage with no involvement of the vermis; 22 (34%) with punctate white matter lesions; and 22 (34%) with diffuse excessively high signal intensity (DEHSI) of the white matter. These mild pathologies are known to be poorly predictive of later neurodevelopmental outcome at the individual level,[31–34] and there were no significant differences in early developmental outcome between the term and preterm-born groups (Table 1).

MRI data acquisition

Neuroimaging was acquired in a single scan session for each infant at the Evelina Newborn Imaging Centre, Evelina London Children's Hospital, using a 3 T Philips Achieva system (Philips Medical Systems). All infants were scanned without sedation in a scanner environment optimized for safe and comfortable neonatal imaging, including a dedicated transport system, positioning device and a customized 32-channel receive coil, with a custom-made acoustic hood.[35] MRI-compatible ear putty and earmuffs were used to provide additional acoustic noise attenuation. Infants were fed, swaddled and comfortably positioned in a vacuum jacket prior to scanning to promote natural sleep. All scans were supervised by a neonatal nurse and/or paediatrician who monitored heart rate, oxygen saturation and temperature throughout the scan.

Table 1 Research participants

Group	(i) Term-born infants scanned at 43.5–44.5 weeks PMA (n = 24)	(ii) Term-born infants scanned at 37–43.5 weeks PMA (n = 248)	(iii) Preterm-born infants scanned at 37–43.5 weeks PMA (n = 65)	(ii) versus (iii)	
				Test statistic	P
Female (%)	13 (54)	114 (46)	26 (40)	0.742[a]	0.389
GA at birth, median (range), weeks	40.9 (38.9–42)	40 (37–42.3)	31.9 (24.3–36.9)	12.409[b]	< 0.001
Weight at birth, median (range), kg	3.77 (2.75–4.33)	3.34 (2.1–4.8)	1.64 (0.54–4.1)	10.959[b]	<0.001
Orbitofrontal circumference at birth, median (range), cm	35 (33.5–37)	34.5 (30.5–38)	29.5 (21–36)	9.576[b]	<0.001
PMA at scan, median (range), weeks	43.9 (43.6–44.4)	40.9 (37.4–43.4)	40.3 (37–43.1)	1.756[b]	0.078
Bayley-III developmental follow-up[c]	20/24 (83%)	207/248 (83%)	53/65 (82%)	0.136[a]	0.712
Cognitive composite standardized score, mean (SD)[c]	101 (10.3)	100 (11.4)	102 (10.5)	1.178[d]	0.240
Communication composite standardized score, mean (SD)[c]	103 (17.2)	96.5 (15.3)	98.7 (16.4)	0.912[d]	0.363
Motor composite standardized score, mean (SD)[c]	100 (10.9)	101 (10.2)	98.9 (9.5)	1.584[d]	0.115

GA = gestational age.

[a]χ^2 test; [b]Z (Mann-Whitney U-test); [c]Bayley Scales of Infant and Toddler Development (Third Edition), performed at around 18 months corrected age; [d]t (unpaired t-test).

Downloaded from https://academic.oup.com/brain/article/144/7/2199/6178274 by Imperial College London Library user on 10 September 2021

High temporal resolution BOLD functional MRI optimized for neonates was acquired over 15 min 3 s (2300 volumes) using a multislice gradient-echo echo planar imaging (EPI) sequence with multiband excitation (multiband factor 9). Repetition time was 392 ms, echo time was 38 ms, flip angle was 34°, and the acquired spatial resolution was 2.15 mm isotropic.[36] For registration of the functional MRI data, high-resolution T_1- and T_2-weighted anatomical imaging was also acquired in the same scan session, with a spatial resolution of 0.8 mm isotropic (T_1-weighted: field of view 145 × 122 × 100 mm, repetition time 4795 ms; T_2-weighted: field of view 145 × 145 × 108 mm, repetition time 12 000 ms, echo time 156 ms).

Functional data preprocessing

Data were preprocessed using an in-house pipeline optimized for neonatal imaging and specifically developed for the dHCP, detailed in Fitzgibbon *et al.*[37] In brief, susceptibility dynamic distortion together with intra- and intervolume motion effects were corrected in each subject using a bespoke pipeline including slice-to-volume and rigid-body registration.[38–41] To regress out signal artefacts related to head motion, cardiorespiratory fluctuations and multiband acquisition,[42] 24 extended rigid-body motion parameters were regressed together with single-subject ICA noise components identified with the FSL FIX tool (Oxford Centre for Functional Magnetic Resonance Imaging of the Brain's Software Library, version 5.0). Denoised data were registered into T_2-weighted native space using boundary-based registration[43] and non-linearly registered to a standard space based on a weekly template from the dHCP volumetric atlas[44] using a diffeomorphic multimodal (T_1/T_2) registration.[45]

While the functional MRI preprocessing pipeline for the dHCP[37] addresses the potential problem of head motion in rs-fMRI data,[46,47] motion is also a surrogate marker of the arousal state of the infant, which interacts with the underlying neural activity.[48,49] To address this issue, we opted for a conservative approach consisting of the selection of a continuous subsample of the data (~70%) with lowest motion for each subject, and excluding those subjects with a high level of motion from further analyses. Specifically, volumes with DVARS (the root mean square intensity difference between successive volumes) >1.5 interquartile range (IQR) above the 75th centile, after motion and distortion correction, were considered as motion outliers.[37] Mean DVARS was 90.5 [standard deviation (SD) 18.5] in the term-born group and 95.5 (SD 20.3) in the preterm-born group ($P = 0.056$, unpaired *t*-test). As DVARS is a relative measure, the absolute DVARS cut-off varied between subjects. Within each acquired dataset (2300 volumes), the continuous set of 1600 volumes with the minimum number of motion-outlier volumes was identified, and the dataset cropped accordingly for all subsequent analyses. Subjects with more than 160 motion-outlier volumes (10% of the cropped dataset) were excluded entirely. This allowed us to minimize the potential effect of different states of arousal even after appropriately denoising the data. The number of motion-outlier volumes remaining in the cropped dataset was recorded for each subject and included as a covariate in all subsequent regression analyses. The median number of motion-outlier volumes in the term-born group was 49.5 (IQR 27–86.5) and in the preterm-born group was 34 (IQR 12–83) [group difference not significant under assumption of normality ($P = 0.185$, unpaired *t*-test) or non-normality ($P = 0.052$, Mann-Whitney U-test)].

Functional data analysis

Group-level network definition

We first defined the normative set of RSNs by group ICA in 24 healthy term-born infants scanned at 43.5–44.5 weeks PMA. These subjects were excluded from all subsequent regression analyses. Probabilistic group ICA by temporal concatenation across subjects was carried out using FSL MELODIC.[30] The ICA dimensionality was set at 30, representing a pragmatic balance between robustness and interpretability (as in Toulmin *et al.*[19]). The output comprised 30 group-average spatial maps representing 30 independent components. The maps were visually inspected and each component manually labelled as RSN or noise, following guidelines in Fitzgibbon *et al.*[37]

Subject-level analyses

We next regressed the group-level spatial maps into the subject-level 4D space-time datasets of the subjects scanned at 37–43.5 weeks PMA (248 term-born, 65 preterm-born). Specifically, the group-level spatial maps (including both RSN signal and artefact components) were used to generate subject-specific versions of the spatial maps and associated time series using dual regression.[50] Artefact components were included to better account for confound variance (noise) in the regression model.[51] First, for each subject, the set of group-level RSN spatial maps was regressed (as spatial regressors in a multiple regression) into the subject's 4D space-time dataset. This resulted in a set of subject-specific time series, one per group-level spatial map. Next, those time series were regressed (as temporal regressors, again in a multiple regression) into the same 4D dataset, resulting in a set of subject-specific spatial maps, one per group-level spatial map.

We then performed cross-subject analysis using general linear models (GLM) to test for the effects of group (term versus preterm birth, sex) and continuous variables (gesational age at birth, PMA at scan) on the subject-level RSN spatial maps, including the number of motion-compromised volumes as a nuisance covariate. Specifically, in the model evaluating the effect of PMA at scan (term-born infants only) the covariates were sex and motion; in the model evaluating the effect of sex the covariates were PMA at scan, gesational age at birth and motion; in the model evaluating the effect of term versus preterm birth the covariates were PMA at scan, sex and motion; and in the model evaluating the effect of gesational age at birth the covariates were PMA at scan, sex and motion. A further group-level analysis was conducted in which term-born infants were separated into weekly bins according to their PMA at scan, enabling group-average maps of functional connectivity at each week of brain development to be generated for qualitative comparison. For this we entered data from the 20 subjects in each bin (37.5–38.5 weeks, 38.5–39.5 weeks, 39.5–40.5 weeks, 40.5–41.5 weeks, and 41.5–42.5 weeks) with the lowest number of postnatal days of life at time of scan, to maximize similarity between groups for meaningful visual comparison. The covariates in this model were sex and motion. Voxel-wise statistical tests were implemented in FSL *randomise*[52] using threshold-free cluster enhancement[53] with 5000 permutations. As all contrasts were two-tailed, family-wise error-rate (FWE) corrected (for multiple comparisons across voxels) *P*-values < 0.025 were accepted as significant. Because of the exploratory nature of this study, the main results are presented without correction for the effect of multiple RSNs assessed; however, we also provide the Bonferroni-corrected results (i.e. $P < 0.025/n$ RSNs) in the Supplementary material.

To quantify longitudinal changes in within-network functional connectivity, we analysed the relationship between PMA at scan and a derived parameter we term 'core network strength'. This measure was determined for each RSN for each subject by masking the RSN-specific spatial map (the output of stage two of dual regression) by the corresponding group-ICA network template thresholded at $Z > 3$, then calculating the mean β-parameter value (regression coefficient) within the masked image. The partial Spearman's correlation between core network strength and PMA

Downloaded from https://academic.oup.com/brain/article/144/7/2199/6178274 by Imperial College London Library user on 10 September 2021

at scan was calculated in term-born infants while controlling for sex and motion (number of motion-compromised volumes), and a GLM was used to test for group differences in core network strength between term and preterm infants while controlling for PMA at scan, sex and motion. Correlation and GLM analyses of core network strength were implemented in Python 3.7 with *Pingouin* 0.2.9 and *statsmodels* 0.10.1.

Anatomical localization and data visualization

Results were localized in the standard space using an in-house adaptation of the neonatal version[54] of the AAL atlas,[55] projected to the 40-week high-resolution neonatal dHCP template.[44] Data were displayed using FSLeyes for planar visualization and Connectome Workbench for cortical surface visualization.

Data availability

The dHCP is an open-access project. The imaging and collateral data used in this study were included in the 2019 (second) dHCP data release, which can be downloaded by registering at https://data.developingconnectome.org/.

Results

Resting state networks

Eleven RSNs were identified by group ICA in a subsample of term-born infants scanned between 43.5 and 44.5 weeks PMA ($n = 24$), who were excluded from any further analyses. Five RSNs included primary motor or sensory cortical areas and were categorized as primary networks (Fig. 1A): medial motor, lateral motor, somatosensory, auditory and visual. The remaining six were categorized as association networks (Fig. 1C): motor association (including the premotor and supplementary motor areas), temporoparietal (including Broca's area and the extended Wernicke's area), posterior parietal (including the precuneus and posterior cingulate cortices), frontoparietal (including the frontal, supplementary and parietal eye fields), prefrontal and visual association. The full cortical surface parcellation is provided in Supplementary Fig. 1 and Supplementary Video 1.

Effect of postmenstrual age at scan

To characterize normal maturation in functional connectivity from 37–43.5 weeks in term-born infants, we analysed the association between previously calculated RSNs independently regressed to each subject and PMA at scan, while controlling for sex and motion. Brain regions showing increasing connectivity with older PMA at scan were identified in four RSNs, all association networks (Fig. 2 and Supplementary Fig. 2, Bonferroni-corrected). Localization of significant voxels to the AAL atlas is provided in Supplementary Table 1. There were no brain tissue regions showing negative association with older age at scan.

To illustrate maturational changes in functional connectivity, we produced spatial maps of average network structure in term-born infants categorized into weekly groups according to their PMA at scan, while controlling for sex and motion (Fig. 3).

To quantify longitudinal changes in within-network functional connectivity, we analysed the relationship between PMA at scan and a derived parameter we term 'core network strength', defined as the mean β-parameter value in each subject's RSN-specific spatial map (the outputs of stage two of dual regression) after masking by the corresponding group-ICA network template thresholded at $Z > 3$. Three RSNs showed a positive partial correlation between PMA at scan and core network strength (Fig. 4). There were no RSNs with negative correlation.

Effect of sex

To determine differences in functional connectivity between male and female infants, we analysed this as a group effect, while controlling for gesational age at birth, PMA at scan and motion. Female infants showed increased connectivity of inferior occipitotemporal regions (including the posterior fusiform gyrus) within the visual association network (Fig. 5 and Supplementary Fig. 3, Bonferroni-corrected).

Effect of preterm birth

To determine differences in functional connectivity between term- and preterm-born infants we first analysed this as a group effect, while controlling for PMA at scan, sex and motion. There was extensive impairment of functional connectivity across all RSNs in preterm-born infants; uncorrected core network strength was 23–41% reduced relative to term-born infants across the 11 networks (all $P < 0.001$, independent samples *t*-tests). Conversely, preterm-born infants showed increased connectivity of the bilateral superior parietal lobule within the lateral motor network (Fig. 6 and Supplementary Fig. 4, Bonferroni-corrected). The association of younger gesational age at birth with impaired functional connectivity was replicated across all networks in a separate analysis in which gesational age at birth was entered as a continuous variable, indicating a dose-dependent effect of prematurity on functional connectivity (Supplementary Figs 5 and 6, Bonferroni-corrected).

Discussion

In this large cohort of newborn infants we provide detailed characterization of the maturational trajectories of normal functional network development at TEA, and show that the early developmental disruption imposed by preterm birth is associated with significant and widespread alterations in functional connectivity.

Network architecture and maturation in term-born infants

Overall, we found a robust, modular, symmetrical functional organization of the brain at TEA. Our results confirm and further elucidate the primary-to-higher order maturational sequence of RSN development. Using a whole-brain, voxel-level approach, we depicted changes in the posterior parietal, frontoparietal, prefrontal and visual association networks, showing expansions in network shape with increasing age at scan (Fig. 2). We also investigated the effect of age at scan across a predefined area (the core region, as defined by the template network), demonstrating global changes in network strength or integrity in the somatosensory, posterior parietal and visual association networks (Fig. 4).

Primary networks

We identified five primary RSNs (Fig. 1A), which showed adult-like topology from the earliest ages studied (Fig. 3A) and no significant change in architecture from 37 to 43.5 weeks PMA. Primary, unimodal RSNs mature earlier than higher-order networks in the preterm brain[6,9,56]; our finding of an adult-like configuration of primary RSNs at TEA is in agreement with previous studies at this age.[6–9,11,12,26] The precise localization of sensorimotor networks along the central sulcus is especially striking in our data, even in the youngest infants studied (Fig. 3A). Determination of somatotopic maps in primary sensorimotor cortical areas occurs as early

Downloaded from https://academic.oup.com/brain/article/144/7/2199/6178274 by Imperial College London Library user on 10 September 2021

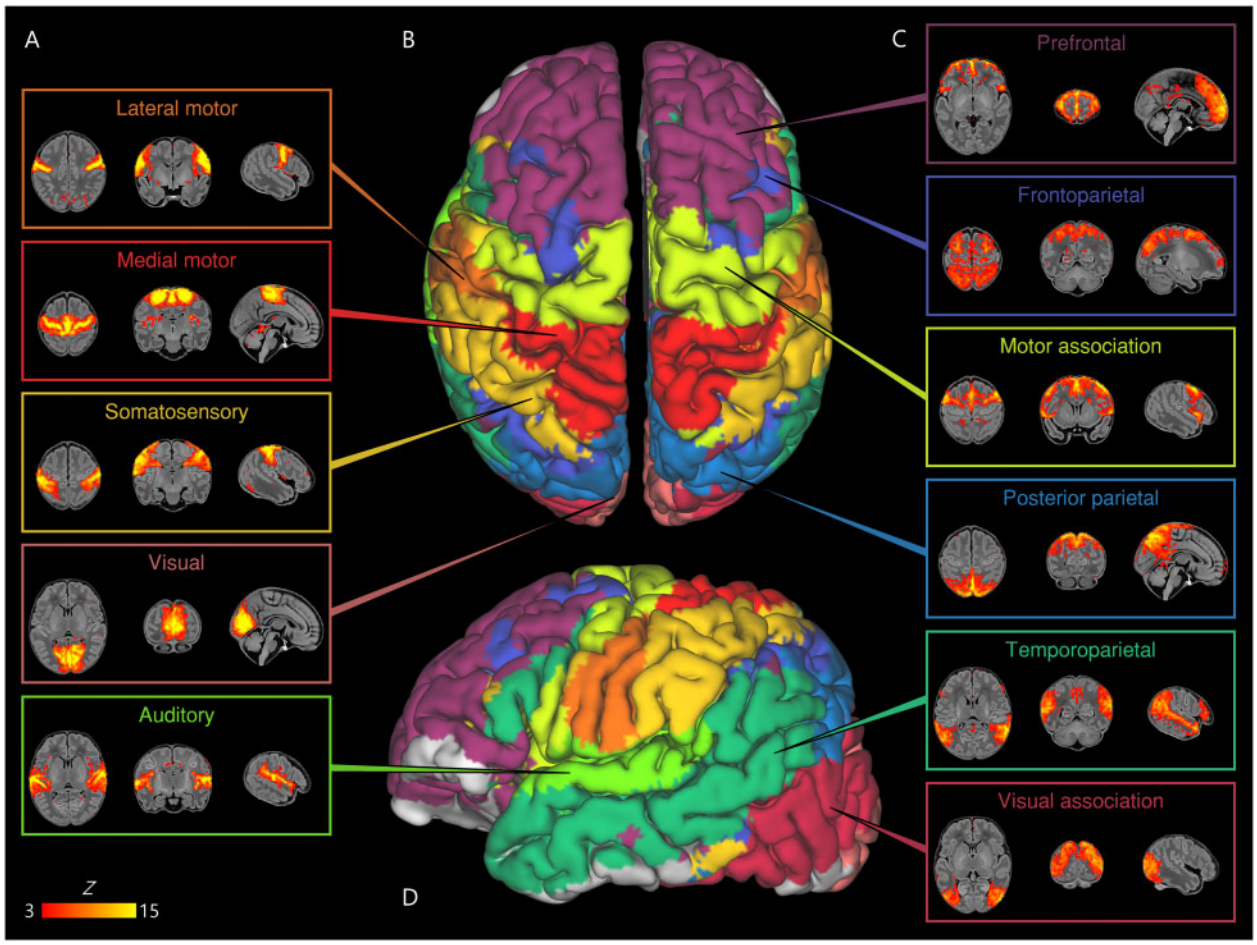

Figure 1 Resting state networks identified by group independent component analysis. Spontaneous BOLD activity patterns (RSNs) derived from group ICA in 24 term-born infants scanned at 43.5–44.5 weeks PMA. *Panels*: Example axial, coronal, and sagittal slices for meaningful spatial patterns in primary (**A**) and association (**C**) RSNs, thresholded at $Z > 3$ and overlaid on a T_1 structural template, displayed in radiological convention. *Centre*: Functional parcellation of the brain using a 'winner-takes-all' approach based on the RSNs from group ICA. RSNs were spatially smoothed and thresholded at $Z > 1$ prior to determination of the 'winning' RSN at each voxel. The resulting volume was projected to the midthickness cortical surface using enclosed (nearest neighbour) volume-to-surface mapping, here displayed on the pial surface of an individual subject scanned at 42 weeks PMA and viewed from the dorsal (**B**) and left lateral (**D**) aspects.

as mid-third trimester equivalent age, with similar stimulation response to adults observed by TEA.[57,58] We additionally observed a significant increase in core network strength within the somatosensory network from 37 to 43.5 weeks PMA (Fig. 4), possibly reflecting increasing integration of secondary somatosensory cortex at this age,[57] and/or increased influence of *ex utero* experience on this network. The bilateral insula (Fig. 1A) and thalamus (Supplementary Fig. 1C) were strongly connected within the medial motor network, consistent with previous studies finding strong thalamocortical connectivity in sensorimotor networks.[10,19]

Association networks

We identified six RSNs representing higher-order association networks (Fig. 1C). Using quantitative (Figs 2 and 4) and qualitative (Fig. 3) methods, we found modest expansions in both the spatial extent and core temporal coherence of higher-order association networks from 37 to 43.5 weeks PMA. To our knowledge this is the first time these changes have been quantified over this brief but developmentally critical period. The heterogeneous timing of functional network development, in which primary networks mature earlier than higher-order association networks, can be related to parallel changes in brain structure (reviewed in Keunen *et al.*[24]). Structural connectivity of the cortex begins with thalamic connections to frontal, auditory, visual and somatosensory cortices at 24–32 weeks gestation, while long-range cortico-cortical connections are not established until 33–35 weeks (reviewed in Dubois *et al.*[59] and Kostovic and Jovanov-Milosevic[60]). The same sequence is later repeated in cortical myelination, with the 'primordial' sensorimotor and visual cortices histologically more mature at the time of birth.[61] White matter tracts connecting to these regions, such as the corticospinal tract and optic radiation, are also the first to mature later in infancy (reviewed in Dubois *et al.*[27]). The structural and functional ontogeny mirrors the observed behavioural sequence of developmental 'milestones' in young children, in which sensorimotor, auditory and visual competencies are acquired before higher-order cognitive functions.[24]

The two RSNs showing greatest increase in intrinsic connectivity (core network strength) from 37 to 43.5 weeks PMA were the posterior parietal network and visual association network (Fig. 4). The former encompasses the medial precuneus and posterior cingulate cortices (Supplementary Fig. 1C), an area of emerging functional connectivity at TEA.[62] In adulthood these regions are a prominent component of the DMN, leading some to label infant RSNs encompassing these as DMN precursors.[6–10] However, the mature DMN also incorporates distinct modules in the anterior cingulate/medial prefrontal cortex, orbitofrontal cortex, lateral

Downloaded from https://academic.oup.com/brain/article/144/7/2199/6178274 by Imperial College London Library user on 10 September 2021

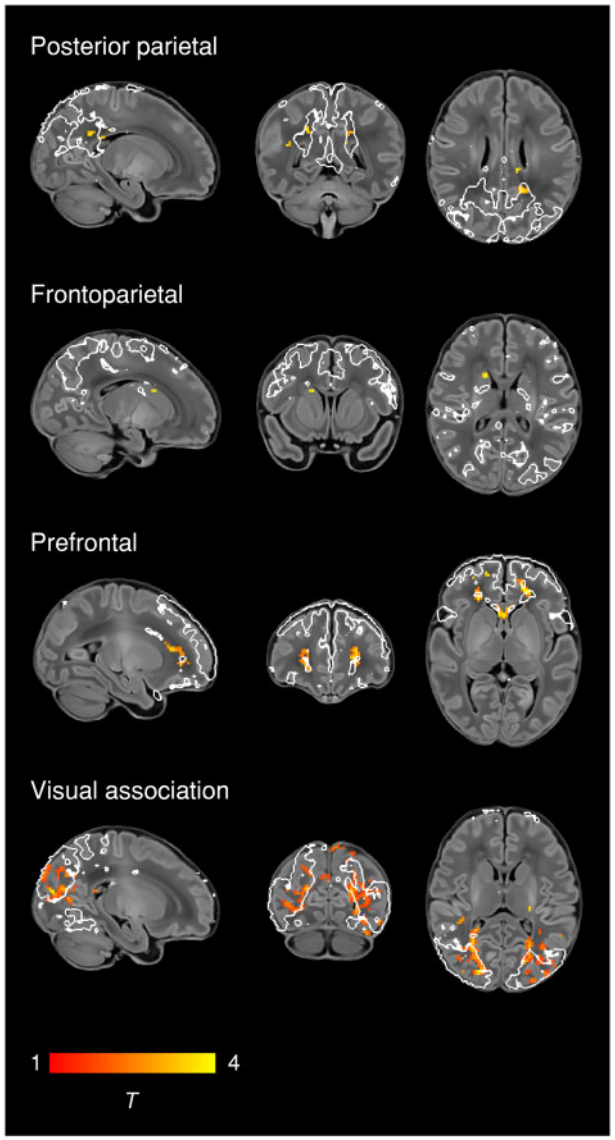

Figure 2 Changes in network shape with increasing age at scan. Brain regions showing increasing functional connectivity with older PMA at scan in term-born infants scanned at 37–43.5 weeks PMA. Example sagittal, coronal, and axial slices for meaningful spatial patterns in four RSNs are shown, overlaid on a T_1 structural template and displayed in radiological convention. T-statistic maps were thresholded at $P < 0.025$ (FWE corrected). White lines represent the outlines of the group ICA RSNs, thresholded at $Z > 3$.

temporal cortex and hippocampus (reviewed in Raichle[63]). We observed no temporal involvement in the posterior parietal network, and only sparse frontal involvement, specifically at the right anterior cingulate (Supplementary Fig. 1C) and bilateral orbitofrontal cortex (Supplementary Fig. 1E). This dominant posterior hub with limited frontoparietal connectivity bears more similarity to the adult DMN under anaesthesia.[64,65] Overall we find support for the concept of fragmented local modules prevailing over long-range integration at this period of development, preceding the emergence of a full analogue of the adult DMN at 6–12 months of age.[11,12,62]

The visual association network comprises lateral occipital (Supplementary Fig. 1D) and inferotemporal (Supplementary Fig. 1B) cortices; regions that contribute to the ventral stream of visual processing, in which simple features coded by primary visual cortex are transformed into higher-level representations of objects, invariant of their size, rotation and position, enabling downstream object recognition and semantic processing.[66,67] It was therefore not surprising to find significant growth in the strength of this network from 37–43.5 weeks PMA (Figs 2 and 4), a period in which infants are increasingly exposed to, and able to resolve, objects in the visual field.[68] Furthermore, after controlling for differences in age, we found areas of increased connectivity within this network in female infants across inferotemporal regions including the posterior fusiform gyrus (Fig. 5). The fusiform is sensitive to complex visual stimuli including faces and facial expressions[69]; in the corresponding region of the macaque brain the code determining face cell firing was recently deciphered.[70] In humans, reduced functional connectivity of the fusiform face area is associated with developmental prosopagnosia.[71] The sex difference in functional connectivity we have identified in this region is especially interesting in the context of behavioural data in which female neonates, compared to males, show increased preference for looking at faces.[72] Sex differences in visual attention to social stimuli have also been described in older infants[73] and in other newborn primates.[74] Structural brain development is sexually dimorphic, with small differences in tissue morphometry observed across the lifespan, frequently involving the temporal lobes, and under the influence of foetal testosterone in males.[75,76] Our finding of a sex difference in functional brain development in the inferior temporal lobes is interesting in this context, although the biological mechanisms for this and any correlations with behavioural data remain unknown at this time. Further investigation of functional connectivity in the ventral stream and social-cognitive development might elucidate mechanisms for sex differences in this domain.

Two RSNs comprised segregated (i.e. non-contiguous) brain regions, revealing anatomically meaningful patterns of functional connectivity. The temporoparietal network (Fig. 1D) connects a posterior module encompassing the extended Wernicke's area to a smaller anterior module corresponding to Broca's area. Integrated structural-functional analysis in adults showed this network is facilitated by the arcuate fasciculus.[77] The instatement of a putative 'language network' in early infancy is supported by stimulus-functional MRI showing activation of these regions in response to speech.[78,79] The frontoparietal network (Fig. 1B) connects the frontal, supplementary and parietal eye fields, with close resemblance to the adult dorsal attention network.[80] Ocular control relies on widespread white matter connections between cortical and subcortical regions, the microstructural integrity of which correlates with visual fixation behaviour in the neonate.[81] Striatal projections of the frontal and supplementary eye fields converge upon the caudate nucleus[82]; we found a positive association between older PMA at scan and functional connectivity of the caudate nucleus within this frontoparietal network (Fig. 2), consistent with active development of the oculomotor corticostriatal system at this age.

Impact of preterm birth

Preterm birth confers a high risk of neurodevelopmental impairment[13,14,16] and psychiatric illness in later life.[15] Pervasive deficiencies and delays in structural brain maturation have been identified in preterm infants scanned at TEA, even in those without focal brain injury, including macrostructural differences in tissue volume and gyrification[29,83–85] and microstructural alterations in both grey and white matter.[86–88] The overall structural network architecture appears unchanged, with preservation or even abnormal strengthening of the rich-club organization of highly connected cortical hubs, at the expense of diminished peripheral

Downloaded from https://academic.oup.com/brain/article/144/7/2199/6178274 by Imperial College London Library user on 10 September 2021

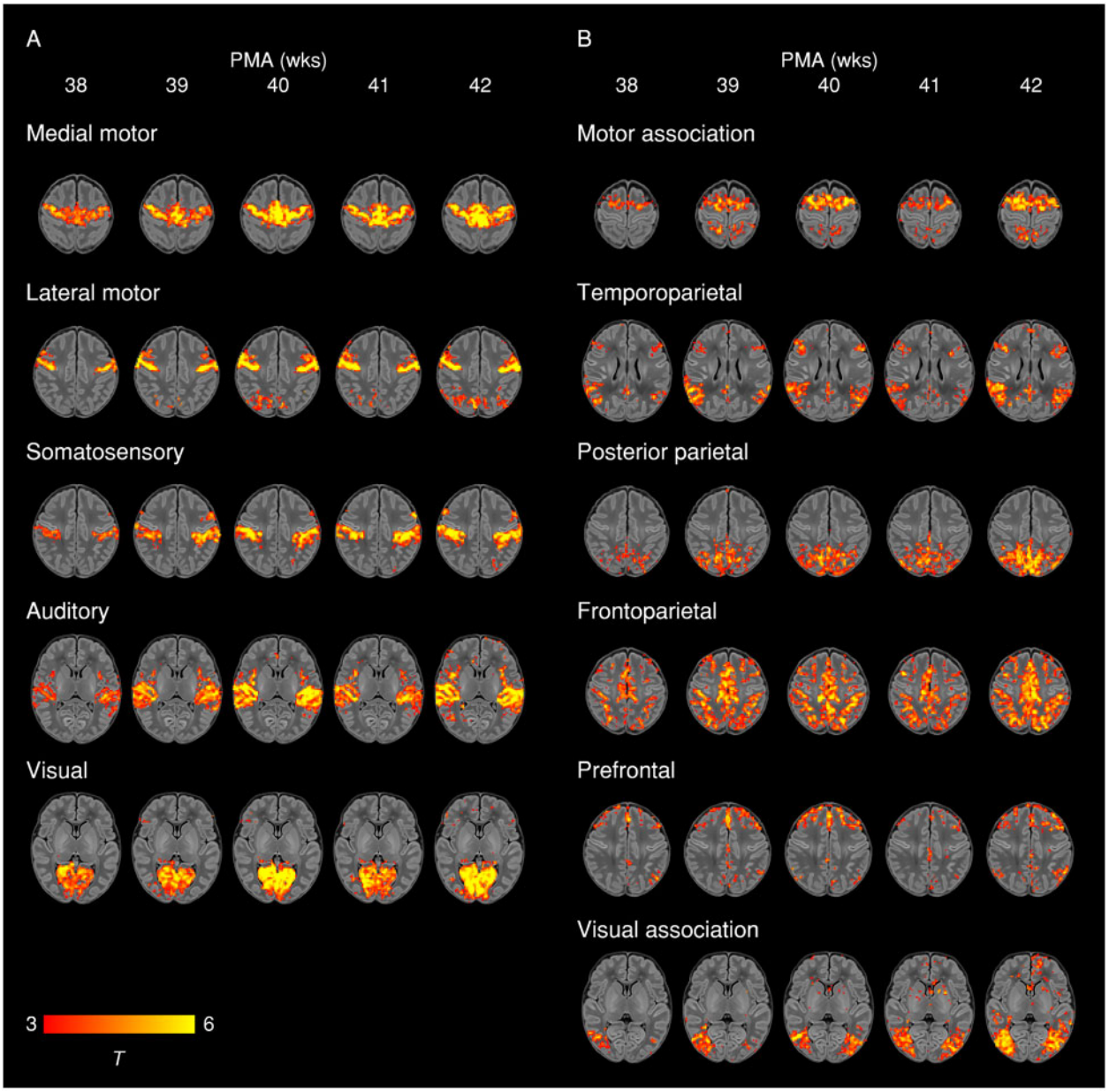

Figure 3 Weekly maturation in functional network structure at term-equivalent age. Group-average *t*-statistic maps of functional connectivity in term-born infants scanned at 37.5–42.5 weeks PMA, grouped into weekly bins by PMA at scan. Within each bin 20 subjects with the lowest postnatal age at time of scan were selected. Example axial slices for meaningful spatial patterns in primary (**A**) and association (**B**) RSNs are shown, overlaid on a T_1 structural template and displayed in radiological convention. Results were thresholded at $P < 0.05$ (FWE corrected).

connectivity and specific disruptions to thalamocortical, cortical-subcortical and short-distance corticocortical connectivity.[89–93]

Widespread impairment of functional connectivity

Now we show that, similar to structural connectivity, functional connectivity is profoundly affected by preterm birth. We found striking deficiencies in within-network connectivity across the full range of RSNs studied (Fig. 6), also replicated as a dose-dependent relationship, such that increased exposure to prematurity (younger gesational age at birth) was associated with decreased functional connectivity (Supplementary Fig. 5); effects we were not powered to detect in a prior study due to a limited number of term-born infants.[6] Our results suggest that although functional connectivity increases across the preterm period,[6,9,10,94,95] it does not reach a normal configuration at TEA. Instead, there appears to be an aberrant developmental trajectory, in which connections between brain regions are reconfigured by premature exposure to the extra-uterine environment. Graph theoretical approaches have shown global network measures of clustering, integration and modularity at TEA are all reduced in preterm infants compared to full-term controls.[18,96] Hypothesis-driven seed-based approaches have identified disrupted thalamocortical connectivity,[9,19] consistent with structural disruption of the same.[91] In our data-driven, whole-brain ICA approach, the main finding was globally reduced within-network functional connectivity. Primary and association RSNs appeared to be similarly affected, in contrast to the findings of Smyser and colleagues,[9] who also used whole-brain correlation mapping, and found primary RSNs were less affected by

Downloaded from https://academic.oup.com/brain/article/144/7/2199/6178274 by Imperial College London Library user on 10 September 2021

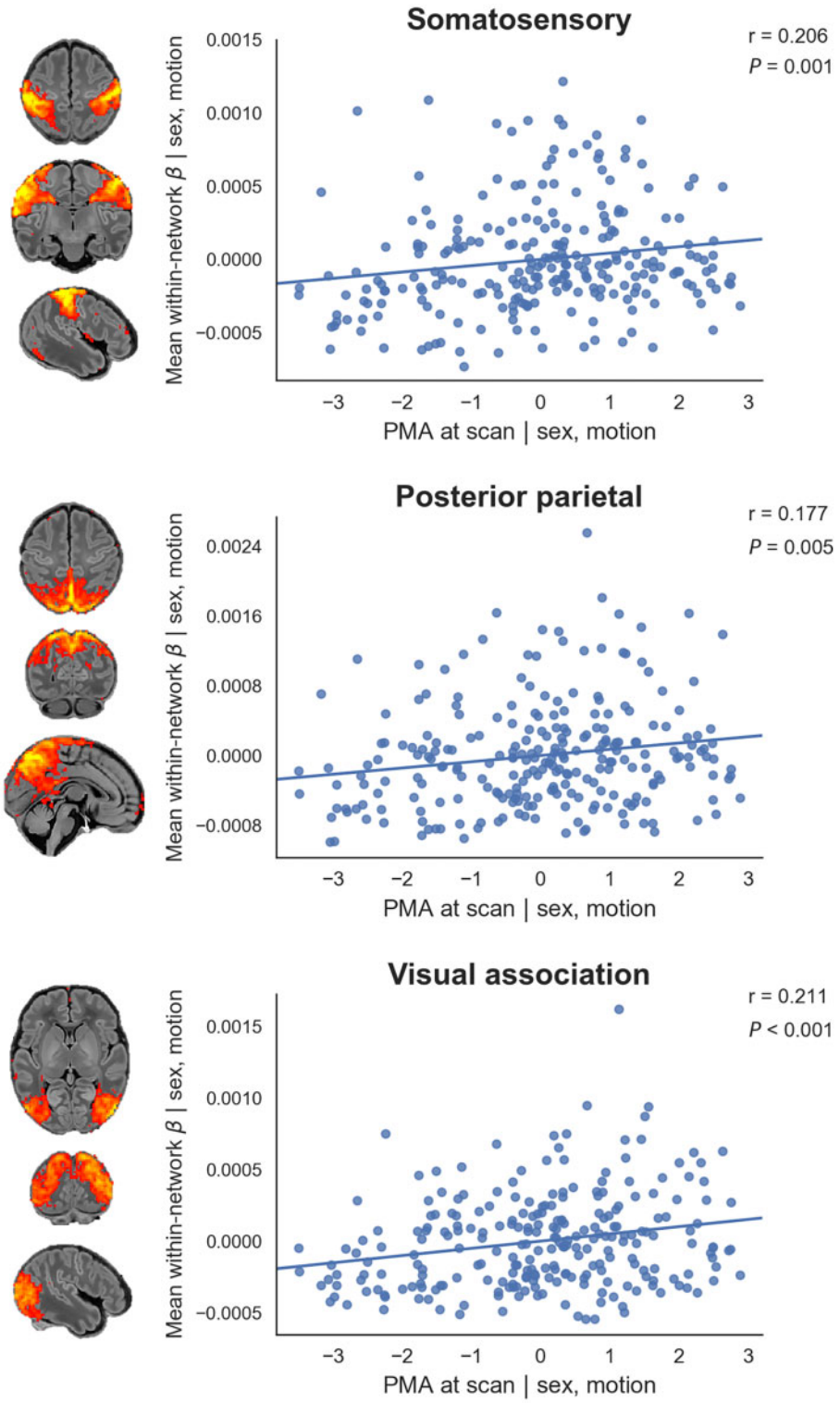

Figure 4 Relationship between postmenstrual age at scan and core network strength. Relationship between the residuals (after correcting for sex and motion) for PMA at scan and core network strength in term-born infants scanned at 37–43.5 weeks PMA. Core network strength was defined as the mean β-parameter value in each subject's RSN-specific spatial map after masking by the corresponding group-ICA network template thresholded at $Z > 3$. Partial Spearman's correlation coefficients and associated *P*-values are displayed for the three RSNs significant at $P < 0.025$. Example axial, coronal and sagittal slices for meaningful spatial patterns in the corresponding group-ICA network templates are shown for reference.

prematurity.[10] This discrepancy may be due to differences in approach to RSN definition (adult-derived RSNs), network mapping (node-based) and inclusion criteria for the preterm group (<30 weeks gesational age at birth). In another study investigating preterm-at-term infants with whole-brain ICA, the method comprised identification of 71 nodes by ICA followed by subject-specific network estimation and selection of discriminatory edges between cases and controls using machine-learning classifiers.[17]

Downloaded from https://academic.oup.com/brain/article/144/7/2199/6178274 by Imperial College London Library user on 10 September 2021

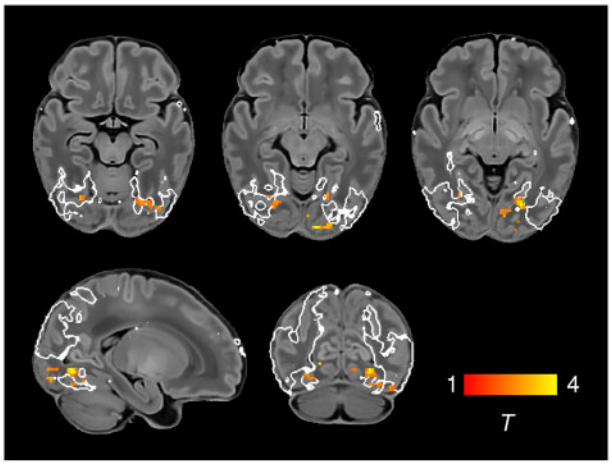

Figure 5 Increased functional connectivity in the visual association network in female infants. Brain regions showing increased functional connectivity within the visual association RSN in female infants. Example axial, sagittal and coronal slices for meaningful spatial patterns are shown, overlaid on a T_1 structural template and displayed in radiological convention. T-statistic maps were thresholded at $P < 0.025$ (FWE corrected). White lines represent the outline of the group-ICA visual association network, thresholded at $Z > 3$.

Connections to frontal and basal ganglia nodes were overrepresented among the discriminatory edges, indicating altered connectivity in preterm infants. Taken together, these different approaches provide complementary demonstrations of spatially widespread impaired RSN coherence in the preterm-at-term brain.

Modulation of parieto-motor connectivity

In the context of brain-wide deficiencies in functional connectivity in preterm-at-term infants, it was notable that there was also increased functional connectivity of the bilateral superior parietal lobule (Brodmann area 5) within the lateral motor network, both when prematurity was evaluated as a group effect (Fig. 6) and as a continuous variable (Supplementary Fig. 5). The lateral motor network corresponds approximately to the primary somatotopic regions serving the upper limb, hand and face (Fig. 1D). *Ex utero* experience during the preterm period strongly influences the development of sensorimotor networks: bilateral functional responses in the peri-rolandic cortices to stimulation of the wrist increase with postnatal age, even after controlling for gesational age at birth.[57] Interestingly, connectivity with superior parietal regions appears to occur as a feature of normal development in the lateral motor network in older term-born infants (Fig. 3A). Brodmann area 5 comprises the somatosensory association cortex, which integrates visual and somatosensory inputs to encode limb configuration in space, enabling coordinated movements within the immediate environment.[97,98] Neural circuits are shaped by experience during critical periods of development; in animal studies, peak plasticity in somatosensory networks occurs earlier than peak plasticity in visual and auditory networks (reviewed in Reh *et al.*[99]). It is intuitive that connectivity of area 5 with lateral motor cortex could be highly dependent upon *ex utero* experience, given the natural constraints upon limb movement and visuomotor integration *in utero*. We propose therefore that the experience of premature exposure to the extrauterine environment, occurring at a time of heightened sensorimotor plasticity,[57,100,101] modulates the normal development of parieto-motor connectivity and leads to an abnormal increase in connectivity at TEA, while acknowledging this mechanistic account as speculative at the present time.

Previous studies have identified increased functional connectivity of certain primary cortical regions in preterm-at-term infants compared to controls, specifically the lateral postcentral gyrus with the thalamus[19] and regional connectivity within occipital/visual networks.[87] This may occur at the expense of connectivity in other brain areas, and can persist into later life; analysis of language networks in preterm children scanned at 12 years of age showed increased connectivity with primary sensorimotor areas, but reduced connectivity with higher-order frontal areas.[102] Relatively conserved topology of core structural networks has been reported in preterm-born babies,[92] persisting into later childhood and adulthood.[103,104] Disruption of the normal balance of sensorimotor development may have persisting effects on later motor and cognitive development. In the mature brain, the superior parietal lobule supports not only the smooth execution of motor plans[105] but also more abstract visuospatial functions such as mental rotation.[106] The aberrant parietal connectivity we have identified at TEA could therefore be a prelude to specific difficulties occurring with high prevalence in preterm children, such as developmental coordination disorder,[107–111] inattention and intellectual impairment (reviewed in Rogers *et al.*[112]). Long-term follow-up of the study population at school age will be required to confirm this hypothesis.

Limitations

The customized neonatal imaging system for the dHCP includes a close-fitting head coil sized specifically for the neonatal head, thus providing exceptional signal-to-noise at the cortical surface.[35] This bias towards surface-proximate sources is compounded by the use of highly accelerated multiband EPI.[37] As such, this has likely resulted in greater sensitivity to detect correlated signal fluctuations in the cerebral cortex compared to deeper sources such as the thalamus, basal ganglia and cerebellum. This may explain the relatively sparse involvement of subcortical regions in the identified RSNs (Fig. 1A and C). Thalamocortical and cerebellar functional connectivity may be better appreciated with seed-based methods.[19,113] We also noted sparse involvement of inferior frontotemporal regions, even at $Z > 1$ (Supplementary Fig. 1B). The dHCP functional pipeline includes advanced distortion-correction techniques,[37] but some signal loss related to air/tissue and bone/tissue interfaces in this vicinity cannot be fully excluded, and our use of a single phase-encode direction (anterior-posterior) may also compress signal in the frontal regions. However, this sparsity may also reflect biological reality in these brain regions, which are the least myelinated at birth[61] and so may be the least able to participate in long-range phase-synchronous activity.

In this study we used a dense sampling strategy at TEA to infer longitudinal change in RSNs, but each infant was scanned on only one occasion. Gesational age at birth and PMA at scan were strongly correlated within the term-born group, which complicates the interpretation of these longitudinal analyses. Furthermore, as some potentially relevant neonatal characteristics, such as intracranial volume and postnatal days of life, are intrinsically associated to some of our variables of interest (i.e. PMA at scan, sex, gesational age at birth), it is difficult to disentangle their relative contributions to our results.

The optimized functional MRI dHCP pipeline includes multiple steps to control for motion and physiological confounds, thus minimizing data loss. However, while well-fed babies tend to fall asleep during the scan, subject motion is inherently correlated with the arousal and sleep state of the baby, which may have an effect in the reconstructed RSNs.[114] While our stringent control for high motion during the scan will minimize the potential effect of subject differences in arousal and sleep state, the specific measure

Downloaded from https://academic.oup.com/brain/article/144/7/2199/6178274 by Imperial College London Library user on 10 September 2021

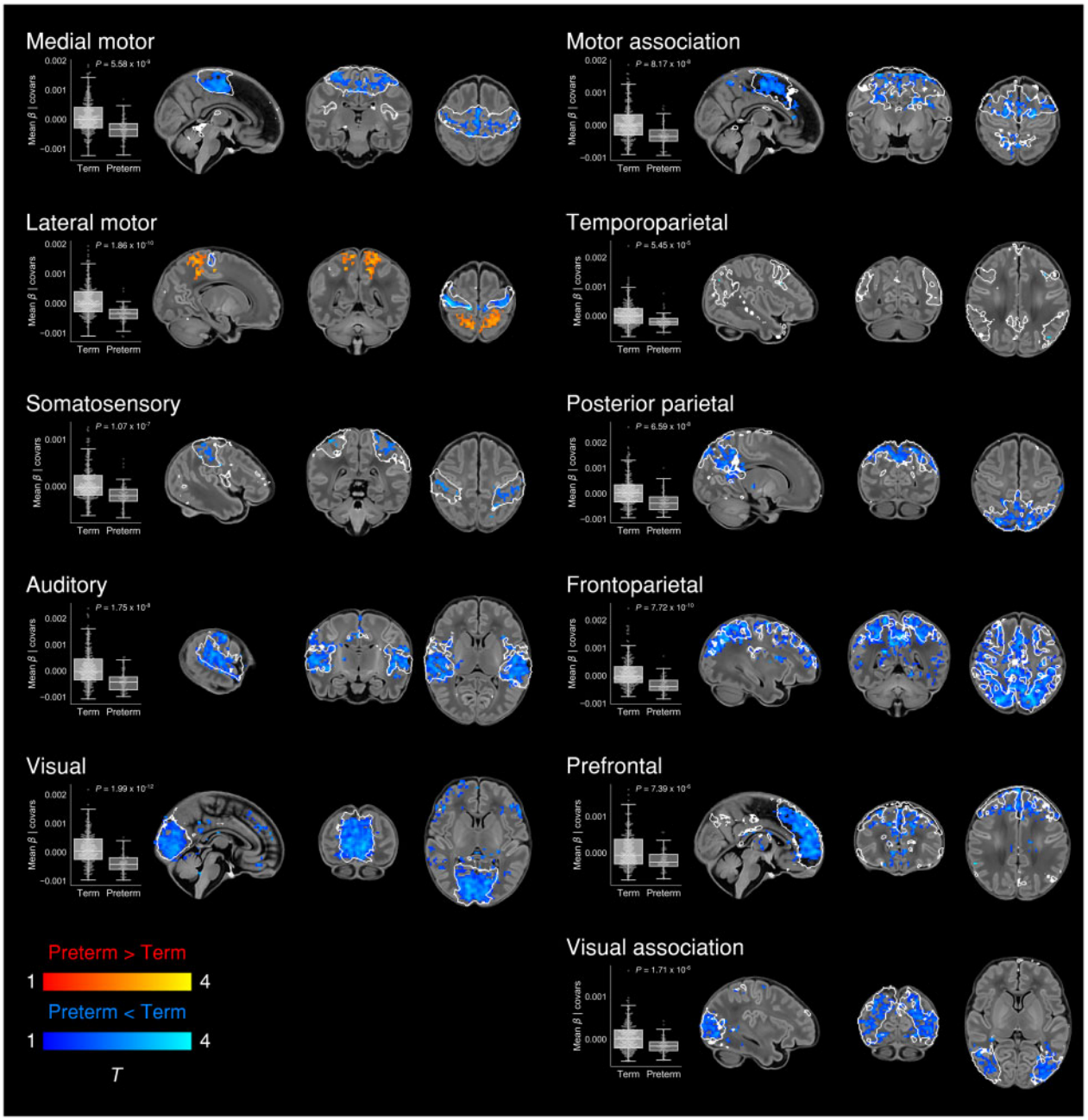

Figure 6 Effect of preterm birth on functional connectivity. Group differences in functional connectivity between term and preterm-born infants scanned at 37–43.5 weeks PMA. Coloured *t*-statistic maps thresholded at $P < 0.025$ (FWE corrected) show brain regions with reduced (blue) or increased (red-yellow) connectivity in preterm-born infants. Example sagittal, coronal, and axial slices for meaningful spatial patterns within each RSN are shown, overlaid on a T_1 structural template and displayed in radiological convention. White lines represent the outlines of the group-ICA RSNs, thresholded at $Z > 3$. Box plots show group differences in core network strength after regressing out PMA at scan, sex and motion. Core network strength was defined as the mean β-parameter value in each subject's RSN-specific spatial map after masking by the corresponding group-ICA network template thresholded at $Z > 3$. *P*-values relate to the term versus preterm group contrast in a GLM in which core network strength was the dependent variable and PMA at scan, sex and motion were controlled for as nuisance covariates.

that should be used as a surrogate to model arousal state is unclear. Future studies using simultaneous EEG-functional MRI could help to better understand the effect of different sleep states on RSNs. Differences in arousal in the scanner between infants and adults should also be considered when comparing RSN topology between these groups.[115] Our use of infants scanned at 43.5–44.5 PMA to define the group-ICA components may have missed some sources of structured noise occurring predominantly at younger ages, such as CSF signal in the cavum septum pellucidum. More fundamentally, the extent to which BOLD signal might be confounded by cerebrovascular factors differing between preterm and term-born infants[116] remains open to debate. Some of the spatial expansions in association RSNs depicted in Fig. 2 were localized to white matter (Supplementary Table 1), which may also reflect maturational changes in cerebrovascular factors, combined with other age-related changes in sulcal depth and white matter signal-to-noise ratio. Some of the important temporal dynamics in functional networks may be missed by rs-fMRI, which predominantly

Downloaded from https://academic.oup.com/brain/article/144/7/2199/6178274 by Imperial College London Library user on 10 September 2021

identifies activity at <0.1 Hz.[3] Complementary approaches such as EEG may help to address this.[117,118]

Conclusion

Brain development occurs in a preprogrammed and spatially heterogeneous progression, modulated by environmental influence. As such, we observed different trajectories for different neural systems, obeying a generally primary-to-higher order sequence of maturation. At TEA we found already instated a complete set of adult-analogous unimodal RSNs corresponding to primary sensorimotor, visual and auditory cortices, with relatively little change from 37–43.5 weeks PMA. In contrast, association RSNs appear fragmented and incomplete compared to the adult repertoire, and are undergoing active maturation at this time. Connectivity within the visual association network in particular is highly associated with age, likely as a result of postnatal environmental experience, but also modified by the sex of the infant. Preterm birth is associated with profoundly reduced functional connectivity across all RSNs, but also with augmentation of parieto-motor connectivity, with possible implications for understanding certain neurocognitive sequelae of prematurity. In future we may be able to positively modulate RSN development in prematurity via targeted environmental manipulations.[119] Preterm birth is best conceptualized as a developmental perturbation that reconfigures, rather than simply diminishes, the organization of functional brain networks.

Acknowledgements

We thank Shona Falconer, Andrew Chew and Nicholas Harper for providing the Bayley-III developmental follow-up data.

Funding

This work was supported by the European Research Council under the European Union Seventh Framework Programme (FP/2007–2013)/ERC Grant Agreement no. 319456. The authors acknowledge infrastructure support from the National Institute for Health Research (NIHR) Mental Health Biomedical Research Centre (BRC) at South London, Maudsley NHS Foundation Trust, King's College London and the NIHR-BRC at Guys and St Thomas' Hospitals NHS Foundation Trust (GSTFT). The authors also acknowledge support in part from the Wellcome Engineering and Physical Sciences Research Council (EPSRC) Centre for Medical Engineering at King's College London [WT 203148/Z/16/Z] and the Medical Research Council (UK) [MR/K006355/1 and MR/L011530/1]. Additional sources of support included the Sackler Institute for Translational Neurodevelopment at King's College London, the European Autism Interventions (EU-AIMS) trial and the EU AIMS-2-TRIALS, a European Innovative Medicines Initiative Joint Undertaking under Grant Agreements No. 115300 and 777394, the resources of which are composed of financial contributions from the European Union's Seventh Framework Programme (Grant FP7/2007–2013). M.E. was supported by the NIHR-BRC at GSTFT. T.A. was supported by a Medical Research Council (MRC) Clinician Scientist Fellowship [MR/P008712/1]. J.O. and A.D.E. received support from the Medical Research Council Centre for Neurodevelopmental Disorders, King's College London [MR/N026063/1]. J.O. is supported by a Sir Henry Dale Fellowship jointly funded by the Wellcome Trust and the Royal Society [206675/Z/17/Z]. D.B. received support from a Wellcome Trust Seed Award in Science [217316/Z/19/Z]. The views expressed are those of the author(s) and not necessarily those of the NHS, the NIHR or the Department of Health. The funders had no role in the design and conduct of the study; collection, management, analysis, and interpretation of the data; preparation, review, or approval of the manuscript; and decision to submit the manuscript for publication.

Competing interests

The authors report no competing interests.

Supplementary material

Supplementary material is available at *Brain* online.

References

1. Biswal B, Yetkin FZ, Haughton VM, Hyde JS. Functional connectivity in the motor cortex of resting human brain using echo-planar MRI. *Magn Reson Med*. 1995;34(4):537–541.
2. Damoiseaux JS, Rombouts SARB, Barkhof F, et al. Consistent resting-state networks across healthy subjects. *Proc Natl Acad Sci U S A*. 2006;103(37):13848–13853.
3. Cordes D, Haughton VM, Arfanakis K, et al. Frequencies contributing to functional connectivity in the cerebral cortex in "resting-state" data. *AJNR Am J Neuroradiol*. 2001;22(7):1326–1333.
4. De Luca M, Beckmann CF, De Stefano N, Matthews PM, Smith SM. fMRI resting state networks define distinct modes of long-distance interactions in the human brain. *Neuroimage*. 2006;29(4):1359–1367.
5. Raichle ME, MacLeod AM, Snyder AZ, Powers WJ, Gusnard DA, Shulman GL. A default mode of brain function. *Proc Natl Acad Sci U S A*. 2001;98(2):676–682.
6. Doria V, Beckmann CF, Arichi T, et al. Emergence of resting state networks in the preterm human brain. *Proc Natl Acad Sci U S A*. 2010;107(46):20015–20020.
7. Fransson P, Skiold B, Engstrom M, et al. Spontaneous brain activity in the newborn brain during natural sleep–an fMRI study in infants born at full term. *Pediatric Res*. 2009;66(3):301–305.
8. Fransson P, Skiold B, Horsch S, et al. Resting-state networks in the infant brain. *Proc Natl Acad Sci U S A*. 2007;104(39):15531–15536.
9. Smyser CD, Inder TE, Shimony JS, et al. Longitudinal analysis of neural network development in preterm infants. *Cerebr Cortex*. 2010;20(12):2852–2862.
10. Smyser CD, Snyder AZ, Shimony JS, Mitra A, Inder TE, Neil JJ. Resting-state network complexity and magnitude are reduced in prematurely born infants. *Cerebr Cortex*. 2016;26(1):322–333.
11. Gao W, Alcauter S, Elton A, et al. Functional network development during the first year: Relative sequence and socioeconomic correlations. *Cerebr Cortex*. 2014;25(9):2919–2928.
12. Gao W, Alcauter S, Smith JK, Gilmore JH, Lin W. Development of human brain cortical network architecture during infancy. *Brain Struct Funct*. 2015;220(2):1173–1186.
13. Bhutta AT, Cleves MA, Casey PH, Cradock MM, Anand KJ. Cognitive and behavioral outcomes of school-aged children who were born preterm: A meta-analysis. *JAMA*. 2002;288(6):728–737.
14. Marlow N, Wolke D, Bracewell MA, Samara M. Neurologic and developmental disability at six years of age after extremely preterm birth. *N Engl J Med*. 2005;352(1):9–19.
15. Nosarti C, Reichenberg A, Murray RM, et al. Preterm birth and psychiatric disorders in young adult life. *Arch Gener Psychiatry*. 2012;69(6):E1–E8.

Downloaded from https://academic.oup.com/brain/article/144/7/2199/6178274 by Imperial College London Library user on 10 September 2021

16. Saigal S, Doyle LW. An overview of mortality and sequelae of preterm birth from infancy to adulthood. *Lancet*. 2008; 371(9608):261–269.
17. Ball G, Aljabar P, Arichi T, et al. Machine-learning to characterise neonatal functional connectivity in the preterm brain. *Neuroimage*. 2016;124(Pt A):267–275.
18. Bouyssi-Kobar M, De Asis-Cruz J, Murnick J, Chang T, Limperopoulos C. Altered functional brain network integration, segregation, and modularity in infants born very preterm at term-equivalent age. *J Pediatr*. 2019;213:13–21.e1.
19. Toulmin H, Beckmann CF, O'Muircheartaigh J, et al. Specialization and integration of functional thalamocortical connectivity in the human infant. *Proc Natl Acad Sci U S A*. 2015; 112(20):6485–6490.
20. Finn ES, Shen X, Scheinost D, et al. Functional connectome fingerprinting: Identifying individuals using patterns of brain connectivity. *Nat Neurosci*. 2015;18(11):1664–1671.
21. Wang D, Buckner RL, Fox MD, et al. Parcellating cortical functional networks in individuals. *Nat Neurosci*. 2015;18(12): 1853–1860.
22. Glasser MF, Coalson TS, Robinson EC, et al. A multi-modal parcellation of human cerebral cortex. *Nature*. 2016;536(7615): 171–178.
23. Blankenship AG, Feller MB. Mechanisms underlying spontaneous patterned activity in developing neural circuits. *Nat Rev Neurosci*. 2010;11(1):18–29.
24. Keunen K, Counsell SJ, Benders M. The emergence of functional architecture during early brain development. *Neuroimage*. 2017;160:2–14.
25. Vasung L, Abaci Turk E, Ferradal SL, et al. Exploring early human brain development with structural and physiological neuroimaging. *Neuroimage*. 2019;187:226–254.
26. Fransson P, Aden U, Blennow M, Lagercrantz H. The functional architecture of the infant brain as revealed by resting-state fMRI. *Cerebr Cortex*. 2011;21(1):145–154.
27. Dubois J, Dehaene-Lambertz G, Kulikova S, Poupon C, Hüppi PS, Hertz-Pannier L. Hertz-Pannier L. The early development of brain white matter: A review of imaging studies in fetuses, newborns and infants. *Neuroscience*. 2014;276:48–71.
28. Dubois J, Lefèvre J, Angleys H, et al. The dynamics of cortical folding waves and prematurity-related deviations revealed by spatial and spectral analysis of gyrification. *Neuroimage*. 2019; 185:934–946.
29. Shimony JS, Smyser CD, Wideman G, et al. Comparison of cortical folding measures for evaluation of developing human brain. *Neuroimage*. 2016;125:780–790.
30. Beckmann CF, Smith SM. Probabilistic independent component analysis for functional magnetic resonance imaging. *IEEE Transact Med Imaging*. 2004;23(2):137–152.
31. Broström L, Bolk J, Padilla N, et al. Clinical implications of diffuse excessive high signal intensity (DEHSI) on neonatal MRI in school age children born extremely preterm. *PLoS One*. 2016; 11(2):e0149578.
32. Kersbergen KJ, Benders MJNL, Groenendaal F, et al. Different patterns of punctate white matter lesions in serially scanned preterm infants. *PLoS One*. 2014;9(10):e108904.
33. O'Shea TM, Allred EN, Kuban KCK, et al. Intraventricular hemorrhage and developmental outcomes at 24 months of age in extremely preterm infants. *J Child Neurol*. 2012;27(1):22–29.
34. Steggerda SJ, de Bruïne FT, van den Berg-Huysmans AA, et al. Small cerebellar hemorrhage in preterm infants: Perinatal and postnatal factors and outcome. *Cerebellum*. 2013;12(6):794–801.
35. Hughes EJ, Winchman T, Padormo F, et al. A dedicated neonatal brain imaging system. *Magn Reson Med*. 2017;78(2): 794–804.
36. Price A, Cordero-Grande L, Malik S et al. Accelerated neonatal fMRI using multiband EPI. In: *Proceedings of the 23rd Annual Meeting & Exhibition*. International Society for Magnetic Resonance in Medicine. 2015;23:3911. https://archive.ismrm.org/2015/3911.html
37. Fitzgibbon SP, Harrison SJ, Jenkinson M, et al. The Developing Human Connectome Project (dHCP) automated resting-state functional processing framework for newborn infants. *Neuroimage*. 2020;223:117303.
38. Andersson JLR, Graham MS, Drobnjak I, Zhang H, Campbell J. Susceptibility-induced distortion that varies due to motion: Correction in diffusion MR without acquiring additional data. *Neuroimage*. 2018;171:277–295.
39. Andersson JLR, Graham MS, Drobnjak I, Zhang H, Filippini N, Bastiani M. Towards a comprehensive framework for movement and distortion correction of diffusion MR images: Within volume movement. *Neuroimage*. 2017;152:450–466.
40. Andersson JLR, Hutton C, Ashburner J, Turner R, Friston K. Modeling geometric deformations in EPI time series. *Neuroimage*. 2001;13(5):903–919.
41. Andersson JLR, Skare S, Ashburner J. How to correct susceptibility distortions in spin-echo echo-planar images: Application to diffusion tensor imaging. *Neuroimage*. 2003; 20(2):870–888.
42. Salimi-Khorshidi G, Douaud G, Beckmann CF, Glasser MF, Griffanti L, Smith SM. Automatic denoising of functional MRI data: Combining independent component analysis and hierarchical fusion of classifiers. *Neuroimage*. 2014;90:449–468.
43. Greve DN, Fischl B. Accurate and robust brain image alignment using boundary-based registration. *Neuroimage*. 2009;48(1):63–72.
44. Schuh A, Makropoulos A, Robinson EC, et al. Unbiased construction of a temporally consistent morphological atlas of neonatal brain development. *bioRxiv*. [Preprint] doi:10.1101/251512
45. Avants BB, Epstein CL, Grossman M, Gee JC. Symmetric diffeomorphic image registration with cross-correlation: Evaluating automated labeling of elderly and neurodegenerative brain. *Med Image Analysis*. 2008;12(1):26–41.
46. Power JD, Barnes KA, Snyder AZ, Schlaggar BL, Petersen SE. Spurious but systematic correlations in functional connectivity MRI networks arise from subject motion. *Neuroimage*. 2012; 59(3):2142–2154.
47. Satterthwaite TD, Wolf DH, Loughead J, et al. Impact of in-scanner head motion on multiple measures of functional connectivity: Relevance for studies of neurodevelopment in youth. *Neuroimage*. 2012;60(1):623–632.
48. Denisova K. Neurobiology, not artifacts: Challenges and guidelines for imaging the high risk infant. *Neuroimage*. 2019;185: 624–640.
49. Whitehead K, Laudiano-Dray MP, Meek J, Fabrizi L. Emergence of mature cortical activity in wakefulness and sleep in healthy preterm and full-term infants. *Sleep*. 2018;41(8):zsy096.
50. Nickerson LD, Smith SM, Öngür D, Beckmann CF. Using dual regression to investigate network shape and amplitude in functional connectivity analyses. *Front Neurosci*. 2017;11:115.
51. Beckmann CF, Mackay CE, Filippini N, Smith SM. *Group comparison of resting-state FMRI data using multi-subject ICA and dual regression*. San Francisco: Organisation for Human Brain Mapping; 2009.
52. Winkler AM, Ridgway GR, Webster MA, Smith SM, Nichols TE. Permutation inference for the general linear model. *Neuroimage*. 2014;92:381–397.
53. Smith SM, Nichols TE. Threshold-free cluster enhancement: Addressing problems of smoothing, threshold dependence and localisation in cluster inference. *Neuroimage*. 2009;44(1): 83–98.

Downloaded from https://academic.oup.com/brain/article/144/7/2199/6178274 by Imperial College London Library user on 10 September 2021

54. Shi F, Yap P-T, Wu G, et al. Infant brain atlases from neonates to 1- and 2-year-olds. *PLoS One*. 2011;6(4):e18746.
55. Tzourio-Mazoyer N, Landeau B, Papathanassiou D, et al. Automated anatomical labeling of activations in SPM using a macroscopic anatomical parcellation of the MNI MRI single-subject brain. *Neuroimage*. 2002;15(1):273–289.
56. Liu WC, Flax JF, Guise KG, Sukul V, Benasich AA. Functional connectivity of the sensorimotor area in naturally sleeping infants. *Brain Res*. 2008;1223:42–49.
57. Allievi AG, Arichi T, Tusor N, et al. Maturation of sensorimotor functional responses in the preterm brain. *Cerebr Cortex*. 2015;26(1):402–413.
58. Dall'Orso S, Steinweg J, Allievi AG, Edwards AD, Burdet E, Arichi T. Somatotopic mapping of the developing sensorimotor cortex in the preterm human brain. *Cerebr Cortex*. 2018; 28(7):2507–2515.
59. Dubois J, Adibpour P, Poupon C, Hertz-Pannier L, Dehaene-Lambertz G. MRI and M/EEG studies of the white matter development in human fetuses and infants: Review and opinion. *Brain Plast*. 2016;2(1):49–69.
60. Kostovic I, Jovanov-Milosevic N. The development of cerebral connections during the first 20-45 weeks' gestation. *Sem Fetal Neonatal Med*. 2006;11(6):415–422.
61. Flechsig P. Developmental (myelogenetic) localisation of the cerebral cortex in the human subject. *Lancet*. 1901;158(4077): 1027–1030.
62. Gao W, Zhu H, Giovanello KS, et al. Evidence on the emergence of the brain's default network from 2-week-old to 2-year-old healthy pediatric subjects. *Proc Natl Acad Sci U S A*. 2009; 106(16):6790–6795.
63. Raichle ME. The brain's default mode network. *Ann Rev Neurosci*. 2015;38:433–447.
64. Amico E, Gomez F, Di Perri C, et al. Posterior cingulate cortex-related co-activation patterns: A resting state fMRI study in propofol-induced loss of consciousness. *PLoS One*. 2014;9(6):e100012.
65. Bonhomme V, Vanhaudenhuyse A, Demertzi A, et al. Resting-state network-specific breakdown of functional connectivity during ketamine alteration of consciousness in volunteers. *Anesthesiology*. 2016;125(5):873–888.
66. DiCarlo JJ, Zoccolan D, Rust NC. How does the brain solve visual object recognition? *Neuron*. 2012;73(3):415–434.
67. Goodale MA, Milner AD. Separate visual pathways for perception and action. *Trends Neurosci*. 1992;15(1):20–25.
68. Dubowitz LM, Mushin J, Morante A, Placzek M. The maturation of visual acuity in neurologically normal and abnormal newborn infants. *Behav Brain Res*. 1983;10(1):39–45.
69. Li Y, Richardson RM, Ghuman AS. Posterior fusiform and mid-fusiform contribute to distinct stages of facial expression processing. *Cerebr Cortex*. 2019;29(7):3209–3219.
70. Chang L, Tsao DY. The code for facial identity in the primate brain. *Cell*. 2017;169(6):1013–1028.e14.
71. Lohse M, Garrido L, Driver J, Dolan RJ, Duchaine BC, Furl N. Effective connectivity from early visual cortex to posterior occipitotemporal face areas supports face selectivity and predicts developmental prosopagnosia. *J Neurosci*. 2016;36(13): 3821–3828.
72. Connellan J, Baron-Cohen S, Wheelwright S, Batki A, Ahluwalia J. Sex differences in human neonatal social perception. *Infant Behav Dev*. 2000;23(1):113–118.
73. Alexander GM, Wilcox T, Woods R. Sex differences in infants' visual interest in toys. *Arch Sex Behav*. 2009;38(3):427–433.
74. Simpson EA, Nicolini Y, Shetler M, Suomi SJ, Ferrari PF, Paukner A. Experience-independent sex differences in newborn macaques: Females are more social than males. *Sci ReP*. 2016;6:19669.
75. Lombardo MV, Ashwin E, Auyeung B, et al. Fetal testosterone influences sexually dimorphic gray matter in the human brain. *J Neurosci*. 2012;32(2):674–680.
76. Studholme C, Kroenke CD, Dighe M. Motion corrected MRI differentiates male and female human brain growth trajectories from mid-gestation. *Nat Commun*. 2020;11(1):3038.
77. O'Muircheartaigh J, Jbabdi S. Concurrent white matter bundles and grey matter networks using independent component analysis. *Neuroimage*. 2018;170:296–306.
78. Dehaene-Lambertz G, Dehaene S, Hertz-Pannier L. Functional neuroimaging of speech perception in infants. *Science*. 2002; 298(5600):2013–2015.
79. Dehaene-Lambertz G, Hertz-Pannier L, Dubois J, et al. Functional organization of perisylvian activation during presentation of sentences in preverbal infants. *Proc Natl Acad Sci U S A*. 2006;103(38):14240–14245.
80. Vossel S, Geng JJ, Fink GR. Dorsal and ventral attention systems: Distinct neural circuits but collaborative roles. *Neuroscientist*. 2014;20(2):150–159.
81. Stjerna S, Sairanen V, Gröhn R, et al. Visual fixation in human newborns correlates with extensive white matter networks and predicts long-term neurocognitive development. *J Neurosci*. 2015;35(12):4824–4829.
82. Parthasarathy H, Schall J, Graybiel A. Distributed but convergent ordering of corticostriatal projections: Analysis of the frontal eye field and the supplementary eye field in the macaque monkey. *J Neurosci*. 1992;12(11):4468–4488.
83. Ball G, Boardman JP, Rueckert D, et al. The effect of preterm birth on thalamic and cortical development. *Cerebr Cortex*. 2012;22(5):1016–1024.
84. Kapellou O, Counsell SJ, Kennea N, et al. Abnormal cortical development after premature birth shown by altered allometric scaling of brain growth. *PLoS Med*. 2006;3(8):e265.
85. Keunen K, Kersbergen KJ, Groenendaal F, Isgum I, de Vries LS, Benders MJ. Brain tissue volumes in preterm infants: Prematurity, perinatal risk factors and neurodevelopmental outcome: A systematic review. *J Matern Fetal Neonat Med*. 2012; 25 (Suppl 1):89–100.
86. Ball G, Srinivasan L, Aljabar P, et al. Development of cortical microstructure in the preterm human brain. *Proc Natl Acad Sci U S A*. 2013;110(23):9541–9546.
87. Bouyssi-Kobar M, Brossard-Racine M, Jacobs M, Murnick J, Chang T, Limperopoulos C. Regional microstructural organization of the cerebral cortex is affected by preterm birth. *Neuroimage Clin*. 2018;18:871–880.
88. Krishnan ML, Dyet LE, Boardman JP, et al. Relationship between white matter apparent diffusion coefficients in preterm infants at term-equivalent age and developmental outcome at 2 years. *Pediatrics*. 2007;120(3):e604–e609.
89. Ball G, Aljabar P, Zebari S, et al. Rich-club organization of the newborn human brain. *Proc Natl Acad Sci U S A*. 2014;111(20): 7456–7461.
90. Ball G, Boardman JP, Aljabar P, et al. The influence of preterm birth on the developing thalamocortical connectome. *Cortex*. 2013;49(6):1711–1721.
91. Ball G, Pazderova L, Chew A, et al. Thalamocortical connectivity predicts cognition in children born preterm. *Cerebr Cortex*. 2015;25(11):4310–4318.
92. Batalle D, Hughes EJ, Zhang H, et al. Early development of structural networks and the impact of prematurity on brain connectivity. *Neuroimage*. 2017;149:379–392.
93. Lee JY, Park HK, Lee HJ. Accelerated small-world property of structural brain networks in preterm infants at term-equivalent age. *Neonatology*. 2019;115(2):99–107.

Downloaded from https://academic.oup.com/brain/article/144/7/2199/6178274 by Imperial College London Library user on 10 September 2021

94. Cao M, He Y, Dai Z, et al. Early development of functional network segregation revealed by connectomic analysis of the preterm human brain. *Cerebr Cortex*. 2016;27(3):1949–1963.
95. van den Heuvel MP, Kersbergen KJ, de Reus MA, et al. The neonatal connectome during preterm brain development. *Cerebr Cortex*. 2015;25(9):3000–3013.
96. Scheinost D, Kwon SH, Shen X, et al. Preterm birth alters neonatal, functional rich club organization. *Brain Struct Funct*. 2016;221(6):3211–3222.
97. Graziano MS, Cooke DF, Taylor CS. Coding the location of the arm by sight. *Science*. 2000;290(5497):1782–1786.
98. Mountcastle VB, Lynch JC, Georgopoulos A, Sakata H, Acuna C. Posterior parietal association cortex of the monkey: Command functions for operations within extrapersonal space. *J NeuroPhysiol*. 1975;38(4):871–908.
99. Reh RK, Dias BG, Nelson CA, et al. Critical period regulation across multiple timescales. *Proc Natl Acad Sci U S A*. 2020; 117(38):23242–23251.
100. Arichi T, Counsell SJ, Allievi AG, et al. The effects of hemorrhagic parenchymal infarction on the establishment of sensori-motor structural and functional connectivity in early infancy. *Neuroradiology*. 2014;56(11):985–994.
101. Staudt M. Reorganization after pre- and perinatal brain lesions. *J Anatomy*. 2010;217(4):469–474.
102. Schafer RJ, Lacadie C, Vohr B, et al. Alterations in functional connectivity for language in prematurely born adolescents. *Brain*. 2009;132(3):661–670.
103. Fischi-Gomez E, Muñoz-Moreno E, Vasung L, et al. Brain network characterization of high-risk preterm-born school-age children. *Neuroimage Clin*. 2016;11:195–209.
104. Karolis VR, Froudist-Walsh S, Brittain PJ, et al. Reinforcement of the Brain's Rich-Club architecture following early neurodevelopmental disruption caused by very preterm birth. *Cerebr Cortex*. 2016;26(3):1322–1335.
105. Simon O, Mangin JF, Cohen L, Le Bihan D, Dehaene S. Topographical layout of hand, eye, calculation, and language-related areas in the human parietal lobe. *Neuron*. 2002;33(3): 475–487.
106. Gogos A, Gavrilescu M, Davison S, et al. Greater superior than inferior parietal lobule activation with increasing rotation angle during mental rotation: An fMRI study. *NeuroPsychol*. 2010;48(2):529–535.
107. Caravale B, Herich L, Zoia S, et al. Risk of developmental coordination disorder in Italian very preterm children at school age compared to general population controls. *Eur J Paediatr Neurol*. 2019;23(2):296–303.
108. Davis NM, Ford GW, Anderson PJ, Doyle LW. Developmental coordination disorder at 8 years of age in a regional cohort of extremely-low-birthweight or very preterm infants. *Dev Med Child Neurol*. 2007;49(5):325–330.
109. Dewey D, Thompson DK, Kelly CE, et al. Very preterm children at risk for developmental coordination disorder have brain alterations in motor areas. *Acta Paediatr*. 2019;108(9):1649–1660.
110. Kashiwagi M, Iwaki S, Narumi Y, Tamai H, Suzuki S. Parietal dysfunction in developmental coordination disorder: A functional MRI study. *NeurorePort*. 2009;20(15):1319–1324.
111. Wilson PH, Smits-Engelsman B, Caeyenberghs K, et al. Cognitive and neuroimaging findings in developmental coordination disorder: New insights from a systematic review of recent research. *Dev Med Child Neurol*. 2017;59(11):1117–1129.
112. Rogers CE, Lean RE, Wheelock MD, Smyser CD. Aberrant structural and functional connectivity and neurodevelopmental impairment in preterm children. *J Neurodev Disord*. 2018; 10(1):38.
113. Herzmann CS, Snyder AZ, Kenley JK, Rogers CE, Shimony JS, Smyser CD. Cerebellar functional connectivity in term- and very preterm-born infants. *Cerebr Cortex*. 2018;29(3):1174–1184.
114. Horovitz SG, Braun AR, Carr WS, et al. Decoupling of the brain's default mode network during deep sleep. *Proc Natl Acad Sci U S A*. 2009;106(27):11376–11381.
115. Mitra A, Snyder AZ, Tagliazucchi E, et al. Resting-state fMRI in sleeping infants more closely resembles adult sleep than adult wakefulness. *PLoS One*. 2017;12(11):e0188122.
116. Bouyssi-Kobar M, Murnick J, Brossard-Racine M, et al. Altered cerebral perfusion in infants born preterm compared with infants born full term. *J Pediatrics*. 2018;193:54–61.e2.
117. Arichi T, Whitehead K, Barone G, et al. Localization of spontaneous bursting neuronal activity in the preterm human brain with simultaneous EEG-fMRI. *Elife*. 2017;6:e27814.
118. Mehrkanoon S. Discovering dynamic functional networks in the human neonatal brain with electric source imaging. *bioRxiv*. [Preprint] doi:10.1101/545616.
119. Lordier L, Meskaldji D-E, Grouiller F, et al. Music in premature infants enhances high-level cognitive brain networks. *Proc Natl Acad Sci U S A*. 2019;116(24):12103–12108.

Downloaded from https://academic.oup.com/brain/article/144/7/2199/6178274 by Imperial College London Library user on 10 September 2021